

Chemically Functional Alkanethiol Derivatized Magnetic Nanoparticles

David A. Fleming, Michael Napolitano, Mary Elizabeth Williams*
The Pennsylvania State University, Department of Chemistry,
152 Davey Laboratory, University Park, PA, 16802, U.S.A.

ABSTRACT

Chemically functional magnetic nanoparticles, comprised of an Fe core encased in a thin Au shell, have been prepared by sequential high temperature decomposition of organometallic compounds in a coordinating solvent. A novel approach to encapsulate the Fe core in Au has been developed. TEM analysis confirms that the nanoparticles are monodisperse (~20%) with average diameters of 8nm. The nanoparticles were subsequently functionalized with alkanethiolate ligands, which prevent aggregation, enable solubility in a range of solvents (both hydrophobic and hydrophilic), and permit subsequent derivatization (*e.g.*, via ligand exchange reactions). The functionalized particles are characterized using high-resolution transmission electron microscopy (HRTEM), X-ray powder diffraction (XRD) and ultraviolet-visible (UV-Vis) absorption spectroscopy.

We have utilized place-exchange to impart chemical functionality to the nanoparticles by attaching either (1) thiol-derivatized redox moieties (*e.g.*, ferrocene) or (2) alkanethiols with terminal reactive groups such as alcohols, amines and carboxylic acids. This paper presents our preliminary investigations of the voltammetry of the former class of these magnetic core/shell nanoparticles.

INTRODUCTION

The preparation and characterization of novel nanometer scale materials has led to an exponential increase in research activity concerned with examination of the fundamental properties and potential applications of these materials. Metal nanoparticles, for example, have been applied to innovative applications ranging from electronics¹ and optics² to DNA sensing³ and catalysis.⁴ The utility of magnetic nanoparticles has recently been described⁵ and demonstrated in a few cases for ultrahigh density information data storage,⁶ contrast agents in medical imaging technologies⁷, and 'spintronics'⁸ (*i.e.*, spin-based data transfer and storage). For example, Co and FePt nanoparticles have been shown to be useful for the preparation of highly ordered three-dimensional magnetic superlattices.⁹ There have been several demonstrations of the preparation of magnetic particles in the 10 nm – 2 μ m diameter range, comprised of either metal-coated polymeric beads or polymer-coated magnetic particles,¹⁰ which typically lack chemical functionality (*i.e.* synthetic reactivity) or whose electronic or magnetic properties have not been systematically examined. A critical need remains for the synthetic control of their size and composition, and extension of these materials to broader applications requires the design and synthesis of chemically *functional* magnetic nanoparticles.

Several strategies have been developed for the synthesis of magnetic nanoparticles, most notably those reported by Murray *et al.*, which rely on the thermal decomposition of small organometallic precursors in the presence of stabilizing ligands.¹¹ Using similar methods,

bimetallic particles of, for example, CoPt and FePt have been created, which are limited almost exclusively to alloys. Examples of non-alloyed, heterometallic nanoparticles include noble metal core/shell particles synthesized via citrate reduction¹² and semiconductor core/semiconductor shell materials.¹³ Shells on other particles, in particular magnetic nanoparticles, have yet to be widely reported. We have developed a synthetic strategy that relies on the surface passivation of ferromagnetic Fe particles with a shell Au. The Au shell prevents oxidation of the Fe core, while facilitating nanoparticle functionalization via well-known Au-thiol coupling chemistry. In this paper, we describe a route for the creation of Fe/Au core/shell nanoparticles by the high temperature decomposition of Fe(CO)₅, followed by the subsequent addition of an Au shell via a transmetallation reaction.

Functionalization of *non*magnetic nanoparticles has been demonstrated by the covalent attachment of protective ligand monolayers; these studies have primarily investigated alkanethiolate attachment to Au,¹⁴ Ag,¹⁵ or Pt¹⁶ metal clusters, although many additional ligands have been utilized. Importantly, alkanethiolate monolayers (1) prevent irreversible particle aggregation, (2) impart solubility in solvents of varying polarity, and (3) can be used to create chemical functionality. A significant observation of these systems is that precipitation of the particles *prior* to monolayer protection results in irreversible aggregation.^{5a,17} By analogy, modification of the nanoscale magnetic particles requires *in situ* surface modification. Furthermore, ligand-exchange reactions permit the stepwise functionalization of the core/shell nanoparticles. To demonstrate our ability to prepare magnetic nanoparticles with bound reactive and functional groups, we have exchanged alkanethiolate ligands with alkanethiol-modified ferrocene chains, which impart redox activity. We use the well-known electrochemical signal of ferrocene to confirm nanoparticle substitution.

EXPERIMENTAL

Chemicals

Trioctylphosphine oxide (TOPO, Fluka), hexadecylamine (HDA), iron pentacarbonyl, diphenyl ether (DPE), n-butanol, chloroform and methylene chloride (Aldrich) were used as received. Tetrabutylammonium hexafluorophosphate (TBAPF₆, Fluka) was recrystallized from ethyl acetate. Au(acac)PPh₃¹⁸ and ferrocene thiol¹⁹ were synthesized using literature procedures. Ultrapure water (18.2 MΩ) was purified by a Barnstead NANOpure water system.

Synthesis

In a typical synthetic preparation, a 100mL 3-neck flask was fitted with a condenser and thermometer and charged with 2.5 g (6.46 mmol) TOPO and 7 g (29 mmol) HDA. After thoroughly degassing the mixture, the temperature is raised to 250°C under argon. A solution of 0.625g (1.62 mmol) TOPO, 1.75g (7.25 mmol) HDA and 0.14mL (1.06 mmol) Fe(CO)₅ is heated and injected into the TOPO mixture, and stirred for at least an additional 30 min. The temperature is lowered to 200°C, and a solution containing 0.139g (0.25 mmol) Au(acac)PPh₃ in 10mL DPE is added dropwise. The solution is stirred for 30 min, cooled to ~120°C, 30 mL n-butanol is added, and the resulting black solution stirred for 24 hours.

The nanoparticles are isolated and purified by centrifugation (at least three times) from 50/50 ethanol/butanol, followed by dispersion in ethanol and collection on a permanent magnet (at least twice). The collected nanoparticles are dissolved in 2.5M decanethiol in chloroform, stirred for a minimum of 2 days, and collected via centrifugation. The decanethiol ligands are exchanged by stirring the nanoparticles in 32mM ferrocene thiol in chloroform for at least one week, producing a mixed monolayer.²⁰ Confirmation of removal of all excess ferrocene thiol is obtained from a lack of redox response of the decanted solutions during cyclic voltammetry; Fc content decreases with sequential centrifugation steps, and is below the limits of detection (*ca.* 10 nM) after three or four centrifugation cycles.

Measurements

TEM analysis was performed on a JOEL JEM 1200 EXII transmission electron microscope at the Penn State Biological Electron Microscopy Facility. XRD measurements were performed on a Philips PW3040-MPD X-Ray Diffractometer, and UV-Vis measurements were performed on a Cary 500 UV-Visible-Near IR spectrometer.

Cyclic voltammetry was performed using a CH Instruments Model CHI600A potentiostat interfaced with a personal computer. Pt microelectrodes (25 μ m diameter) were created by flame-sealing Pt microwire (Alfa Aesar) in glass capillaries. The sealed ends of the microelectrodes were bent to a 90° angle in the flame, and polished using fine grit sandpaper and sequentially smaller grades of alumina on fine nap polishing cloths (Buehler). The electrodes were sonicated briefly in ethanol prior to use. Pt and Ag wire were used as counter and reference electrodes, respectively. Sample solutions of functionalized particles (~1mg/ml) in 0.2M TBAPF₆ in chloroform were degassed, and the electrochemical cell sealed, to minimize oxygen contamination.

RESULTS AND DISCUSSION

Nanoparticle Characterization

The size and composition of the nanoparticles were confirmed using transmission electron microscopy (TEM); a representative TEM image of the synthesized Fe core/Au shell nanoparticles is shown in Figure 1A. Analysis shows that the as-prepared samples are relatively monodisperse (~20%) with an average size of 8.25 ± 1.8 nm. Darker, *ca.* 1 nm thick, rings around each particle are attributed to the Au shell, and have near-uniform thicknesses. The polydispersity of the core/shell particles is comparable to that of the Fe cores (prior to capping with Au), indicating that particle polydispersity arises during the initial Fe particle formation.

Further confirmation of nanoparticle structure is obtained from x-ray powder diffraction (XRD) spectra, such as in Figure 1B, which show peaks characteristic of the (111), (200), (220), (311), and (222) lattice planes of fcc Au. Due to similarities in lattice parameters, peaks corresponding to crystalline Fe are obscured by the Au peaks; however, no peaks for Fe oxides are observed as would be expected for Fe cores with protected surfaces. The magnetic character of the particles (evidenced by their attraction to the permanent magnet on which they are collected), taken together with the TEM and XRD data, confirms their Fe core/Au shell structures. High resolution TEM and energy dispersive x-ray spectroscopy studies are underway to gather additional and definitive evidence.

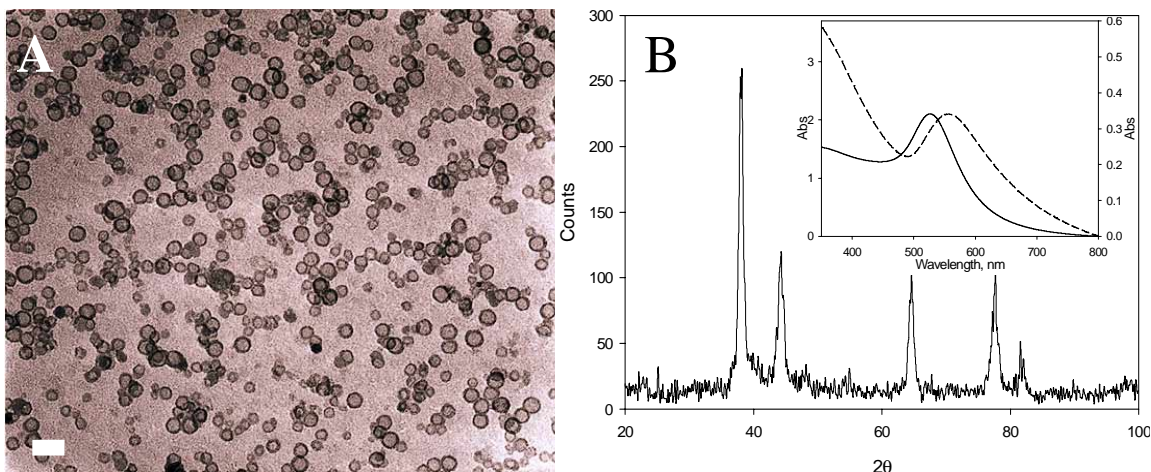


Figure 1. (A) TEM image of 8.25 ± 1.8 nm Fe@Au nanoparticles. Scale bar represents 20nm. (B) XRD spectra showing peaks (from left to right) for (111), (200), (220), (311), and (222) Au lattice planes. The Fe peaks are obscured by the Au (200), (220), and (222) peaks. The inset shows a typical UV-Vis spectrum of Fe@Au nanoparticles (dashed) versus to monometallic Au particles (solid) of similar size.

It is well established that metal nanoparticles possess a characteristic absorption in the visible region of the electromagnetic spectrum due to the surface propagation of free electrons in the metal. The energy of the surface plasmon band is a function of the metal, solvent, attached ligand, and size of the particle, thus is a sensitive measure of the dielectric properties of the nanoparticle. A typical UV-Vis spectrum of the Fe core/Au shell containing a decanethiol monolayer is shown in the inset of Figure 1B. The plasmon band of the Fe@Au nanoparticles appears at 555 nm, and is red-shifted in comparison with monometallic Au nanoparticles of similar size. The energy for the plasmon band may be shifted to lower energy by particle aggregation or due to electronic interaction of the Au shell with the Fe core. We do not observe any decreased solubility, and TEM images show individually isolated particles, so that the shifted plasmon peak cannot be a result of particle aggregation. It has been shown¹² for other core/shell nanoparticles that the energy of the plasmon absorbance of the shell can be dramatically effected by the size and dielectric properties of the core, and we infer that the Fe core causes a similar effect in our materials. Additional studies of the size and composition-dependent plasmon absorption of our alkanethiol stabilized Fe core/Au shell nanoparticles will be reported separately.

Electrochemical Measurements

There have been several reports of electrochemical studies of Au nanoparticles with redox-active ligands;²¹ we analogously attach alkanethiol-modified ferrocenes to the Au shell of our nanoparticles. Figure 2A shows a representative cyclic voltammogram of a solution of Fc-derivatized Fe core/Au shell nanoparticles, and the peak at 0.86 V (vs. Ag/Ag⁺) corresponds to the oxidation of nanoparticle-bound ferrocenes. The forward (oxidation) wave is nearly sigmoidal in shape, consistent with the microelectrode geometry and freely diffusing Fc-modified nanoparticles. However, upon reversing the potential sweep, the return (reduction)

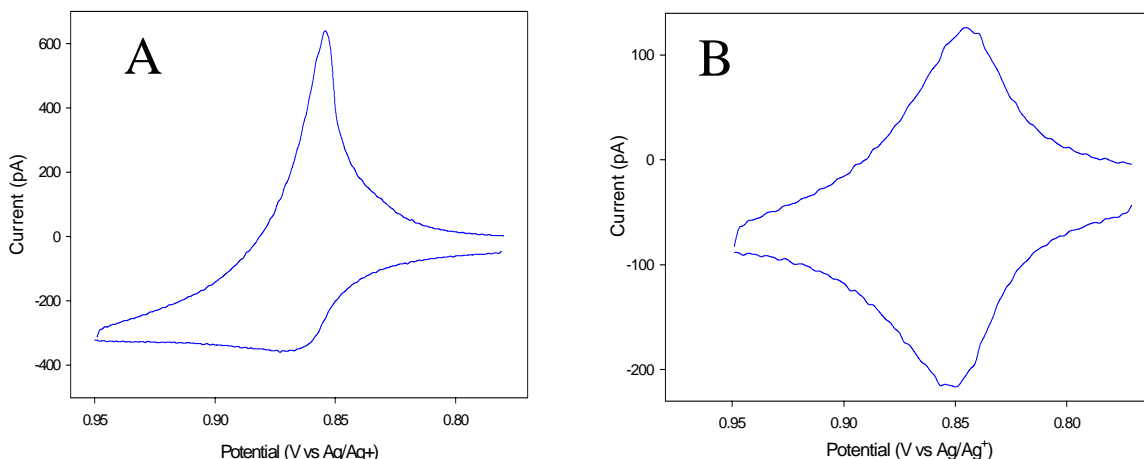


Figure 2. Cyclic voltammograms of (A) solution of Fc-functionalized nanoparticles and (B) microelectrode immersed in an electrolyte solution after nanoparticle adsorption. All voltammograms were performed using a potential scan rate of 20mV/s in 0.2M TBAPF₆ in methylene chloride at a 25 μ m diameter Pt electrode.

wave is sharp and Gaussian, evidence for adsorption of the nanoparticles on the microelectrode surface.

Nanoparticle adsorption was further examined (after these cyclic voltammograms) by removing the microelectrode and re-immersing it in a solution containing only electrolyte; Figure 2B shows a voltammogram of the microelectrode with adsorbed Fc-modified nanoparticles. The difference in potential between the anodic and cathodic peaks (ΔE_p) is 4 mV and the reduction current is five fold smaller. The shape of the redox wave in Figure 2B is consistent with surface-confined redox species on the working electrode.²² The surface coverage, calculated from the integrated current under the oxidation peak, is 1.9×10^{-9} mol/cm². This value is much larger than expected for a single adsorbed layer of nanoparticles, but because the number of ferrocenes per nanoparticle is not known, we are unable to estimate the thickness of the adsorbed particle layer.

CONCLUSIONS

Surface-protected Fe@Au nanoparticles have been synthesized using a novel high temperature approach, and their structure confirmed using TEM, XRD and UV-Visible spectroscopy. The nanoparticles were functionalized with electroactive Fc alkanethiolate ligands and their preliminary voltammetric behavior has been examined. The nanoparticles adsorb to the microelectrode surface, producing redox-active layers.

ACKNOWLEDGEMENTS

This work is funded in part by a grant from the American Chemical Society Petroleum Research Fund Type G grant. We are grateful for additional financial support from the Penn State Department of Chemistry and Eberly College of Science. We thank the Mallouk group for use of the XRD instrumentation.

REFERENCES.

1. Shipway, A. N.; Katz, E.; Willner, I. *Chem. Phys. Chem.* **2000**, *1*, 18-52.
2. For example, (a) Xia, Y.; Gates, B.; Yin, Y.; Lu, Y. *Adv. Mat.* **2000**, *12*, 693-712. (b) Haynes, C. L.; Van Duyne, R. P. *J. Phys. Chem. B.* **2001**, *105*, 5599-5611.
3. Recent examples include: (a) Taton, T. A.; Lu, G.; Mirkin, C. A. *J. Am. Chem. Soc.* **2001**, *123*, 5164-5165. (b) Dubertret, B.; Calame, M.; Libchaber, A. *J. Nat. Biotechnol.* **2001**, *19*, 365-370.
4. (a) Crooks, R. M.; Zhao, M. Q.; Sun, L.; Chechik, V.; Yeung, L. K. *Acc. Chem. Res.* **2001**, *34*, 181-190. (b) Somorjai, G. A.; Borodko, Y. G. *Catal. Lett.* **2001**, *76*, 1-5.
5. (a) Schmid, G. in Clusters and Colloids, from Theory to Applications; VCH Publishers: Weinheim, 1994. (b) Ji, T.; Lirtsman, V. G.; Avny, Y.; Davidov, D. *Adv. Mater.* **2001**, *13*, 1253-1256.
6. (a) Ross, C. *Annu. Rev. Mat. Sci.* **2001**, *21*, 203-235. (b) Tsunashima, S. *J. Phys. D – Appl. Phys.* **2001**, *34*, R87-R102. (c) Kirk, K. J. *Contemp. Phys.* **2000**, *41*, 61-78. (d) Weller, D.; Doerner, M. F. *Annu. Rev. Mat. Sci.* **2000**, *30*, 611-644.
7. (a) Reynolds, C. H.; Annan, N.; Beshash, K.; Huber, J. H.; Shaber, S. H.; Lenkinski, R. E.; Wortman, J. A. *J. Am. Chem. Soc.* **2000**, *122*, 8940-8945. (b) Goldstein, H.; Lumma, W.; Rudzik, A. *Annu. Rep. Med. Chem.* **1989**, *24*, 265-276.
8. Wolf, S. A.; Awschalom, D. D.; Buhrman, R. A.; Daughton, J. M.; von Molnar, S.; Roukes, M. L.; Chtchelkanova, A. Y.; Treger, D. M. *Science*, **2001**, *294*, 1488-1495.
9. (a) Sun, S.; Fullerton, E. E.; Weller, D.; Murray, C. B. *IEEE Trans. Mag.* **2001**, *37*, 1239-1243. (b) Sun, S. H.; Murray, C. B.; Weller, D.; Folks, L.; Moser, A. *Science* **2000**, *287*, 1989-1992.
10. For example, (a) Burke, N. A. D.; Stover, H. D. H.; Dawson, F. P.; Lavers, J. D.; Jain, P. K.; Oka, H. *IEEE Trans. Mag.* **2001**, *37*, 2660-2662. (b) Caruso, F.; Spasova, M.; Susha, A.; Giersig, M.; Caruso, R. A. *Chem. Mater.* **2001**, *13*, 109-116.
11. Murray, C. B.; Sun, S.; Doyle, H.; Betley, T. *MRS Bull.* **2001**, *26*(12), 985-991
12. Kim, Y.; Johnson, R. C.; Li, J.; Hupp, J. T.; Schatz, G. C. *Chem Phys Lett.* **2002**, *352*, 421-428.
13. Reiss, P.; Bleuse, J.; Pron, A. *Nano Lett.* **2002**, *2*, 781-784.
14. The original reports include (a) Brust, M.; Walker, M.; Bethell, D.; Schiffrin, D. J.; Whyman, R. *J. Chem. Soc., Chem. Commun.* **1994**, 801-802. (b) Brust, M.; Fink, J.; Bethell, D.; Schiffrin, D. J.; Kiely, C. *J. Chem. Soc. Chem. Comm.* **1995**, 1655-1656.
15. (a) He, S. T.; Yao, J. N.; Jiang, P.; Shi, D. X.; Zhang, H. X.; Xie, S. S.; Pang, S. J.; Gao, H. J. *Langmuir* **2001**, *17*, 1571-1575.
16. (a) Yee, C.; Scotti, M.; Ulman, A.; White, H.; Rafailovich, M.; Sokolov, J. *Langmuir* **1999**, *15*, 4314-4316.
17. Novak, J. P.; Nickerson, C.; Franzen, S.; Feldheim, D. L. *Anal. Chem.* **2001**, ASAP.
18. Uson, R.; Laguna, A. *Inorg. Synth.* **1998**, *26*, 85.
19. Chidsey, C. E. D.; Bertozzi, C. R.; Putvinski, T. M.; Mujisce, A. M. *J. Am. Chem. Soc.* **1990**, *112*, 4301-4306.
20. Ingram, R. S.; Hostetler, M. J.; Murray, R. W. *J. Am. Chem. Soc.* **1997**, *119*, 9175-9178.
21. (a) Ingram, R. S.; Murray, R. W. *Langmuir* **1998**, *14*, 4115-4121. (b) Hostetler, M. J.; Green, S. J.; Stokes, J. J.; Murray, R. W. *J. Am. Chem. Soc.* **1996**, *118*, 4212-4213.
- 22 Bard, A; Faulkner, L. R. in Electrochemical Methods: Fundamentals and Applications, 2nd Edition, John Wiley & Sons, Inc.: New York, 2001.